HHS Public Access

Author manuscript

Cancer Lett. Author manuscript; available in PMC 2016 September 02.

Published in final edited form as:

Cancer Lett. 2015 April 1; 359(1): 65–74. doi:10.1016/j.canlet.2014.12.052.

Nanoparticle delivery of HIF1α siRNA combined with photodynamic therapy as a potential treatment strategy for head-and-neck cancer

Wei-Hua Chen[a,1], **Rumwald Leo G. Lecaros**[b,1], **Yu-Cheng Tseng**[c], **Leaf Huang**[c,d,e], and **Yih-Chih Hsu**[d,e,f,*]

[a]Graduate Program of Nanotechnology, Chung Yuan Christian University, Taoyuan 32023, Taiwan, ROC

[b]Graduate Program of Bioscience Technology, Chung Yuan Christian University, Taoyuan 32023, Taiwan, ROC

[c]Division of Molecular Pharmaceutics, Eshelman School of Pharmacy, University of North Carolina at Chapel Hill, Chapel Hill, North Carolina 27599, USA

[d]Department of Bioscience Technology, Chung Yuan Christian University, Taoyuan 32023, Taiwan, ROC

[e]Center of Biomedical Technology, Chung Yuan Christian University, Taoyuan 32023, Taiwan, ROC

[f]Center for Nanotechnology, Chung Yuan Christian University, Taoyuan 32023, Taiwan, ROC

Abstract

Combination therapy has become a major strategy in cancer treatment. We used anisamide-targeted lipid–calcium–phosphate (LCP) nanoparticles to efficiently deliver HIF1α siRNA to the cytoplasm of sigma receptor-expressing SCC4 and SAS cells that were also subjected to photodynamic therapy (PDT). HIF1α siRNA nanoparticles effectively reduced HIF1α expression, increased cell death, and significantly inhibited cell growth following photosan-mediated photodynamic therapy in cultured cells. *Intravenous* injection of the same nanoparticles into human SCC4 or SAS xenografted mice likewise resulted in concentrated siRNA accumulation and reduced HIF1α expression in tumor tissues. When combined with photodynamic therapy, HIF1α siRNA nanoparticles enhanced the regression in tumor size resulting in a ~40% decrease in volume after 10 days. Combination therapy was found to be substantially more effective than either HIF1α siRNA or photodynamic therapy alone. Results from caspase-3, TUNEL, and CD31 marker studies support this conclusion. Our results show the potential use of LCP nanoparticles for efficient delivery of HIF1α siRNA into tumors as part of combination therapy along with PDT in the treatment of oral squamous cell carcinoma.

[*]Corresponding author. Tel.: +886 3 265 3522; fax: +886 3 265 3599. ivyhsu@cycu.edu.tw (Y.-C. Hsu).

[1]Wei-Hua Chen and Rumwald Leo G. Lecaros are the co-first authors of equal contribution.

Conflict of interest

The authors declare that they have no conflict of interest.

Keywords

Gene therapy; Drug delivery; Nanoparticle; Gene silencing; Photodynamic therapy

Introduction

Oral and pharyngeal cancer together rank sixth among the most prevalent cancers in the world [1]. Current treatment involves radical surgical excision, chemotherapy and radiotherapy, either separately or in combination. Wide excision of oral cancer can result in facial deformities that impair postsurgical quality of life, underscoring the need to develop new approaches to treatment. Photodynamic therapy (PDT) with systemic or topical administration of photosensitizer is considered to be a non-invasive, well-tolerated alternative as it can be used repeatedly without cumulative side effects, resulting in little or no scar formation [2–5]. This technique is based on the administration of exogenous photosensitizing drugs to render tumor tissue sensitive to non-thermal light of a specific wavelength. The sensitizers are relatively inert and have selective affinity for tumor tissues. In the presence of oxygen, light illumination activates the drug and in turn, through a type II photochemical reaction, produces singlet oxygen which kills tumor cells directly or does so by damage to the tumor-associated vasculature [2,6,7].

Photosan is converted intracellularly into the active photosensitizer, protoporphyrin IX (PpIX), in epithelial cells. PpIX is then activated by 630 nm red light to produce reactive oxygen. Photosanmediated PDT (topical photosan–PDT) has been demonstrated to be an effective treatment modality for oral pre-cancers, however, more than five treatments are needed for relatively large, oral precancerous lesions [8]. In an effort to enhance the therapeutic effect of topical photosan–PDT, we tested a novel approach using calcium phosphate (CaP) based nanoparticle (NP) technology to deliver encapsulated HIF1α siRNA to tumor cells. HIF1α is a hypoxia inducible factor and plays a pivotal role in tumorigenesis, especially in the regulation of apoptosis and cell cycle progression. CaP is not only biocompatible and biodegradable, it also binds nucleic acids with high affinity. It dissolves in the acidic pH of the endosome, increasing osmotic pressure resulting in rupture of the endosome and subsequent release of cargo into the cytoplasm. We stabilized CaP cores with dioleoylphosphatydic acid (DOPA) and further coated them with a cationic lipid. The final NP presents as a hollow spherical structure ranging from 25 to 30 nm in diameter and possess an asymmetric lipid bilayer at the surface. Using the ligand anisamide (AA), lipid–calcium–phosphate (LCP) can efficiently deliver siRNA to sigma receptor-expressing tumor cells to stimulate a strong RNAi effect. With an interest in developing improved therapeutic strategies for oral cancers, we conducted experiments in both cultured cells and xenograft tumors in nude mice to determine if inhibition of HIF1α expression by siRNA nanoparticles would enhance the cell-killing efficacy of topical photosan–PDT.

Materials and methods

Materials

1,2 – Distearoryl – sn – glycero – 3 – phosphoethanolamine – N – [methoxy (polyethyleneglycol-2000) ammonium salt (DSPE-PEG2000), dioleoylphosphatidic acid (DOPA) and 1,2-dioleoyl-3-trimethylammonium-propane chloride salt (DOTAP) were purchased from Avanti Polar Lipids, Inc. (Alabaster, AL). DSPE–PEG–anisamide (AA) was synthesized in our lab as described previously. Texas Red labeled double-stranded oligonucleotide (oligo), with the same siRNA sequence [9], was purchased from Integrated DNA Technologies (Coralville, IA). Other chemicals were obtained from Sigma-Aldrich (St. Louis, MO) without further purification. Human squamous cell carcinoma cells, SCC4 were purchased from Bioresource Collection and Research Center (BCRC; Hsinchu, Taiwan, ROC) and SAS was a gift from Professor Liu, Yang Ming University. Both SCC4 and SAS cells were derived from human tongue with expressing sigma receptors and were used as model cells in our study, SCC4 or SAS cells are cultured at 37°C in a humidified 5% CO_2 and 95% air incubator in DMEM/F12 medium (Invitrogen, Grand Island, NY, US) supplemented with 10% fetal bovine serum (Invitrogen, Grand Island, NY, US). When cells reached 80% confluence, the cells were removed with 0.05% trypsin–EDTA (Invitrogen) and were replated in DMEM/F12 medium. HIF1α siRNA (target sequence: 5′-AGA GGU GGA UAU GUG UGG GdTdT-3′) [9] and scrambled siRNA target sequence: 5′-AUG UAU UGG CCU GUA UUAG-3′) were purchased from Dharmacon (Lafayette, CO, USA) and Texas Redlabeled control siRNA was purchased from Dharmacon (Lafayette, CO, USA) in unprotected, desalted, annealed form. All sequences were adopted from published studies. Photosan was kindly sponsored by SeeLab (Wesselburenerkoog, Germany).

PDT light source

A portable innovative LED light source (Wonder Light, MedEx Healthcare Inc., Taoyuan, Taiwan) was used for PDT treatment of SCC4 xenograft nude mouse tumors. A user-friendly interface of this LED light source coupled with optical fiber was designed and used for the light treatment. The light source consists of a high-power LED, with the wavelength centered at 640 nm and a bandwidth of 20 nm. The power density of the Wonder Light system was tunable, ranging from 1 to 400 mW/cm^2. The size of the light spot is 1.8 cm in diameter at a working distance of 1 cm. The power density was set at 320 mW/cm^2 and the light energy dosage was 100 J/cm^2 [10].

Formulation of LCP encapsulated HIF1α siRNA

LCP was prepared as described previously with slight modifications [11,12]. The target moiety of LCP surface is anisamide to recognize sigma receptors on the surface of SCC4 or SAS. Briefly, 300 μl of 2.5 M $CaCl_2$ with 12 μg of siRNA was dispersed in a 20 ml oil phase (cyclohexane/Igepal CO-520 (71/29, v/v)) to form a well-dispersed water-in-oil reverse microemulsion. The phosphate micro-emulsion was prepared by dispersing 300 μl of 12.5 mM Na_2HPO_4 in a separate 20 ml oil phase. 100 μl (20 mM) of DOPA in chloroform was added to the phosphate solution. After mixing the above two microemulsions for 20 min, 40 ml of ethanol was added to the combined solution and the mixture was centrifuged. After three cycles of ethanol wash, the CaP core pellets were dissolved in chloroform. To prepare

the final LCP, 500 μl of CaP core was mixed with 75 μl of 10 mM DOTAP, 10 mM cholesterol, 3 mM DSPE-PEG-2000 and 3 mM DSPE–PEG–AA. After evaporating the chloroform, the residual lipid was hydrated in 200 μl of 5% glucose to form LCP.

Particle size and charge measurements

Particle size and zeta potential of the final LCP were measured by a Malvern NanoSizer series (Westborough, MA). Transmission Electron Microscope (TEM) images of LCP NP were acquired using TECNAI F20, Philips TEM (FEI Company, Eindhoven, The Netherlands).

Western blot analyses of HIF-1α and sigma receptor

Excised tumors were homogenized and lysed in the lysis buffer using PRO-PREP™ protein extraction solution. Samples containing an equal quantity of protein, as determined by BCA Protein Assay Kit (Pierce, Thermo Fisher Scientific Inc., Rockford, IL, US), were denatured in the sample buffer by boiling at 100 °C for 5 min. Prepared samples were resolved on a 5%/12% Bis-Tris acrylamide gel along with molecular size markers. SDS-PAGE electrophoresis was carried out at a constant voltage (150 V) at room temperature. Proteins were electrophoretically transferred to a nitrocellulose (NC) membrane (Whatman GmbH, Dassel, Germany) at 4 °C at constant 300 mA for 2 h. Following the transfer, the NC blot was blocked with Block PRO blocking buffer (Visual Protein Biotechnology Corporation, Taiwan), incubated with rabbit primary antibodies against hypoxia inducible factor-1α (HIF-1α, 120 kDa; GenTex, Taipei, Taiwan, ROC) (1:1000 dilution), and sigma receptor (SIGMAR1, 25 kDa; GenTex, Taipei, Taiwan, ROC) (1:1000 dilution), respectively, followed by peroxidase-conjugated goat anti-rabbit IgG (GenTex) (1:10,000 dilution), and developed in enhanced chemiluminescence substrate (PerkinElmer, Inc., Boston, MA, USA). Glyceraldehyde 3-phosphate dehydrogenase (GAPDH; GenTex) (1:1000 dilution) was used as an internal control. Intensities of hybridized protein bands on western blots were semi-quantified by VisionWorkers LS software and blots were scanned using an imaging system (BioDoc-It 220, UVP®, Upland, CA, US).

In vitro cellular uptake study of targeting on sigma receptor

SCC4 or SAS cells (3×10^4 cells/well/0.5 ml) were seeded in 24-well plates 16 h before experimentation. Cells were treated with different formulations containing 100 nM Texas Red-DNA oligos in the culture medium at 37 °C for 4 h. SCC4 or SAS cells were washed three times with PBS followed by incubation with 300 μl lysis buffer (0.3% Triton X-100 in PBS) at 37 °C for 0.5 h. The fluorescence intensity of 100 μl cell lysate was determined by an IVIS reader (λex: 595 nm, λem: 613 nm) (IVIS Lumina II, Perkin Elmer Caliper Life Sciences, Hopkinton, MA). For free ligand competition study of the sigma receptor, either SCC4 or SAS cells were co-incubated with 50 μM haloperidol with different formulations.

In vitro cellular study of nontargeted and targeted LCP uptake

SCC4 cells (2×10^4 per well) were seeded in 6-well plates (Corning Inc., Corning, NY) with cover glass for 12 h before the experiment. Cells were treated with different formulations at a concentration of 100 nM Texas Red labeled DNA oligos in serum containing medium at

37 °C for 4 h. After washing twice with PBS, cells were fixed with 4% paraformaldehyde in PBS at room temperature for 1 hr, and then treated with 0.1% Triton X-100 in PBS for 30 min at 37 °C, counterstained with DAPI nuclei acid stain for nuclei staining for 5 min (Molecular Probe, Invitrogen, Eugene, OR, USA), WGA (Wheat Germ Agglutinin Conjugates) for membrane staining for 10 min (Molecular Probes, Invitrogen, Eugene, OR, USA) and were monitored and imaged using an Eclipse C1 plus, Confocal Microscope at 200× magnification (Nikon, Tokyo, JP).

Cell viability analysis by MTT assay

SCC4 cells (5×10^3 per well) were seeded in 24-well plates with 500 μl of DMEM-F12 medium containing 10% fetus bovine serum per well. When SCC4 cells were cultured to 70% confluence, cells were then treated with different formulations at a concentration of 100 nM for HIF1α siRNA, or left untreated. After incubating the cells for 48 h, MTT assay was used to evaluate the cell viability. Untreated cells served as the indicator of 100% cell viability. The absorbance was measured at 570 nm using a microplate reader.

Establishment of SCC4 and SAS xenograft mouse models for treatments

Either 5×10^6 SCC4 or SAS cells in 200 μl of medium were injected subcutaneously in the lower back region of female nude mice. Tumor-bearing mice were treated for 3 days at 24 h interval of a total of three times for SCC4 or SAS xenograft model and certain groups of SCC4 bearing mouse were given 10 mg photosan/kg body weight once after siRNA was given. When SCC4 or SAS tumor size reached approximately 500–800 mm^3, SCC4 animals were randomly divided into 5 groups (Table 1A). The 5 treatments of the groups were given by tail vein injection. The dose of LCP control or HIF1α siRNA given to SCC4 or SAS tumor was 0.36 mg/kg respectively [11]. PDT was given using 0.05 mg photosan dissolved in 200 μl PBS/25 g animal by tail vein injection. Tumor sizes were measured daily and the mice were sacrificed on the 11th day. SAS animals were randomly divided into 3 groups (Table 1B). Tumor sizes were measured daily and the mice were sacrificed on the 4th day. Tumor size was determined by caliper measurement. SCC4 and SAS tumors and organs were collected, dissected, and fixed in 10% formalin for further experiments. These studies were approved (Permit Number: 9915) and carried out in strict accordance with the recommendations in the Guide for the Care and Use of the Institutional Animal Care and Use Committee of Chung Yuan Christian University, Chungli, Taoyuan, Taiwan, ROC.

qRT-PCR of HIF1α siRNA knockdown effect

On the 10th day after designed treatments of SCC4 xenograft mouse or the 3rd day after knockdown treatments, the mRNA levels of HIF1 1α in the SCC4 or SAS tumor tissues were also analyzed by using qRT-PCR. A total of 0.05 g of specimens of each group of either SCC4 or SAS tumor tissues were sampled and homogenated using liquid nitrogen to further analyze HIF1α RNA knockdown effect. Total tissue RNA was extracted with an RNAzol® RT (Molecular Research Center Inc., Cincinnati, Ohio, US), and individual cDNAs were synthesized with a RevertAid First Strand cDNA Synthesis Kit (Famantas, Thermo Fisher Scientific Inc., Waltham, MA, US). Realtime quantitative PCR (qPCR) was performed with a Universal Probe Master (Roche, Applied Science, Mannheim, Germany). Reactions were run with a standard cycling program: 50 °C for 2 min, 95 °C for 10 min, 40

cycles of 95 °C for 15 sec, and 60 °C for 1 min, on a real-time PCR system (Applied Biosystems, Foster City, CA, US).

Immunohistochemistry of CD31 and Ki67

CD31 and Ki67 immunohistochemistry was done on paraffin-embedded sections of SCC4 and SAS tumor tissues. For CD31 examination, after fixation with cold acetone for 20 min, samples were incubated with a 1:50 dilution of rat monoclonal anti-mouse CD31 antibody (BD Pharmingen, San Diego, CA) at 4 °C for 1 h followed by incubation with HRP conjugated goat anti-rat IgG antibody (1:200, Santa Cruz Biotechnology, Santa Cruz, CA) for 30 min. For Ki67 examination, a heat mediated antigen retrieval step was performed using 10 mM citrate buffer pH 6.0. Samples were incubated with a 1:200 dilution of rabbit monoclonal anti-mouse Ki67 antibody (ab16667, Abcam (Cambridge, MA)) for 30 min followed by incubation with HRP conjugated anti-rabbit antibody (Cat.#: 4002-1, Epitomics) for 15 min. Visualization was achieved with a DAB detection kit (Pierce, Rockland, IL) using an Olympus BX53 light microscope (Olympus Corp., Tokyo, JP). Multiple (7 images) tumor images of CD31 or Ki67 on high power (400×) of 5 groups were acquired using software image for analysis.

Apoptosis analysis of cleaved caspase-3 and TUNEL

Cleaved caspase-3 immunohistochemistry and terminal deoxyribonucleotide transferase (TdT)-mediated nick-end labeling (TUNEL) staining was performed to detect apoptotic cells in SCC4 tumor tissues of 5 study groups using paraffin-embedded sections of SCC4 tumor tissues. After fixation with cold acetone for 20 min, samples were incubated with a 1:300 dilution of rabbit polyclonal cleaved caspase-3 (Asp175) antibody (#9661, Cell signaling, Danvers, MA, US) at 4 °C for 1 h followed by incubation with HRP conjugated goat anti-rabbit IgG antibody (1:200, Santa Cruz Biotechnology, Santa Cruz, CA) for 30 min. Visualization of cleaved caspase-3 was achieved with a DAB detection kit (Pierce, Rockland, IL). TUNEL assay was performed in 5 study groups using an *in situ* cell death detection kit, POD, TUNEL System (Roche, Basel, Switzerland). This detection kit is based on the detection of single-and double-stranded DNA breaks that occur at the early stages of apoptosis. Cell nuclei with DAB substrate staining were defined as TUNEL-positive nuclei. TUNEL-positive nuclei were monitored. All specimens were examined with an Olympus BX53 light microscope (Olympus Corp., Tokyo, JP). Multiple (7 images) tumor images of cleaved caspase-3 and Tunel on high power (400×) of 5 groups were obtained using software image for analysis.

Toxicity assay

All toxicity was assayed and analyzed using C57BL/6JNarl mouse serum. Cytokines, interleukin-6 (IL-6) and IL-12, were analyzed using mouse serum after the therapeutic dose (0.36 mg/kg) of LCP. Levels of secreted liver biomarkers (aspartate aminotransferase (AST), alanine aminotransferase (ALT), total-Bilirubin (t-Bil)), kidney biomarkers (creatinine, blood urea nitrogen (BUN), calcium and phosphorus), albumin, total protein, globulin, glucose and muscle biomarkers (lactic dehydrogenase and creatine kinase) were assayed using LCP HIF1α siRNA (3 times) treatment of normal C57BL/6JNarl black mice (n = 3).

Statistics

Data are presented as mean values ± SD. The statistical significance was determined by using one way ANOVA.

Results

Inhibition of tumor cell growth in culture

The effect of HIF1α knockdown on the viability of cultured SCC4 cells was determined by MTT assay (Fig. 1). A significantly diminished survival rate ($p < 0.001$) was seen with either HIF1α siRNA alone or the combination of HIF1α siRNA plus PDT when compared to light-only control or PDT treatment alone. Scrambled HIF1α siRNA however, did not significantly affect cell survival rate. Enhanced cell death was observed when HIF1α siRNA and PDT therapy were combined in cultured SCC4 cells (Fig. 1). These findings support the potential use of this combined therapy for the treatment of oral cancers and prompted further investigation *in vivo*.

Characterization of LCP

The CaP–HIF1α siRNA core was stabilized with DOPA, coated with DOTAP, further grafted with DSPE–PEG (non-targeted) or DSPE–PEG–AA (targeted), and then examined for particle size and morphology. CaP cores presented as hollow, spherical structures 20–30 nm in diameter by TEM (Fig. 2A) with an electron transparent outer-ring composed of lipid bilayer. Overall particle size measured 25–30 nm by dynamic light scattering (Fig. 2B, C), consistent with previously reported results [11,12]. The zeta potential of LCP HIF1α siRNA is 45.2 ± 1.7 mV (in triplicates).

In vitro cellular uptake study

To investigate delivery efficiency of our LCP NP formulations, we performed the cellular uptake study using double-stranded (ds) HIF1α oligonucleotides (DNA) labeled with Texas Red dye (ds DNA) in SCC4 or SAS cell lines. The fluorescence intensity of the cell lysate represents the intracellular delivery efficiency for DNA oligonucleotides (oligos, DNA) by a given formulation. As shown in Fig. 3A, cell lysate from SCC4 or SAS cells treated with free Texas Red-HIF1α oligos showed background fluorescence. Those from SCC4 or SAS cells treated with LCP NP formulations with the ligand anisamide (DNA in NP) had significantly higher fluorescence intensities than LCP NP formulations without the ligand anisamide. LCP can efficiently deliver Texas Red-oligos to sigma receptor-expressing tumor cells in both SCC4 and SAS cell lines. Addition of free haloperidol, a known inhibitor of the sigma receptor, significantly reduced the delivery efficiency of LCP NP but not other formulations. In addition, targeted LCP NP showed 2.5-fold or 3.5-fold increased delivery efficiency compared to non-targeted LCP NP in the SCC4 or SAS cell line, respectively. The addition of free haloperidol significantly reduced the delivery efficiency of targeted LCP NP but no other formulations. To understand the sigma receptor of SCC4 and SAS cells, western blot experiments were conducted. Fig. 3B shows that sigma receptor proteins were expressed in both SCC4 and SAS cell lines.

LCP *in vitro* cellular and *in vivo* animal uptake analysis

Sigma receptors are over-expressed in a variety of human tumors suggesting the potential use of anisamide as a ligand for delivery of genes and drugs to the surface of cancer cells. To investigate the use of sigma receptors for specific targeting to oral squamous cancer cell lines (OSCC) and tumors, we used the human SCC4 cell line and PEGylated LCP with anisamide (AA) on the surface. Delivery of targeted and non-targeted LCP to OSCC was measured by cellular uptake of double-stranded (ds) HIF1α oligonucleotides (DNA) labeled with Texas Red (Fig. 3). Most red fluorescence was detectable throughout the cytoplasm 40 min after addition of AA-targeted NP (Fig. 3D). The red fluorescence in the cells treated with untargeted LCP NP appeared either extracellular or as punctate spots inside the cells, indicating the absence of cytosolic delivery of the oligonucleotides (Fig. 3C). Thus, the presence of the AA ligand had led to internalization and cytoplasmic cargo delivery of the LCP in the treated cells.

To confirm *in vivo* uptake, SCC4 tumor bearing nude mice were intravenously injected with AA-targeted Texas Red labeled LCP NP and fluorescence intensity in the tumor and organs was measured after 4 h (Fig. 4). Staining was barely detectable with AA-targeted Texas Red labeled ds DNA LCP NP in the heart, liver, spleen, lung, and kidney. However, we found the tumor region showed the strongest signal. Delivery of HIF1α siRNA to the tumor is expected to result in effective reduction in HIF1α expression.

In vivo therapeutic outcomes of combined treatment

In order to test anti-cancer therapeutic effects of reduced HIF1α expression in xenograft tumors, nude mice were inoculated with SCC4 or SAS OSCC cells and xenografts were allowed to grow to a volume of 500~800 mm^3. Animals were then randomly divided into either three (SAS) or five treatment groups (SCC4) (Fig. 5) and treated with LCP HIF1α siRNA a total of 3 times at 24 h intervals and then given 2 mg/kg body weight of photosan. SCC4 xenograft mice were treated with (1) PBS; (2) scrambled siRNA in LCP; (3) HIF1α siRNA in LCP and photosan (2 mg/kg) without light delivery; (4) HIF1α siRNA in LCP and PBS with light delivery (100 J); (5) HIF1α siRNA in LCP and photosan (2 mg/kg) with light delivery (100 J), respectively. SAS xenograft mice were treated with (1) PBS; (2) scrambled siRNA in LCP; and (3) HIF1α siRNA in LCP, respectively. siRNA dose in all groups was 0.36 mg/kg. Tumor size was measured daily and mice were sacrificed on day 11 (SCC4) or 24 h after the last treatment (SAS). Targeted LCP containing HIF1α siRNA had a significant inhibitory effect on SCC4 tumor size with best results seen on day 7 after combined treatment with PDT ($p < 0.01$) (Fig. 5), with the degree of inhibition ranging from 40% to 85% reduction in tumor volume by day 10 ($p < 0.01$) (Fig. 5). Tumors shrank in size with HIF1α siRNA treatment alone, but grew back quickly in the absence of subsequent PDT. Combined therapy thus extended the tumor reduction effect to a period of at least 7 days of enhanced therapeutic efficacy.

In vivo antitumor therapeutic mechanism

We quantified the degree of RNA knockdown caused by targeted LCP using qRT-PCR on day 10 (SCC4) and one day after treatments were given to SAS mice. HIF1α siRNA formulated in LCP could silence 80–90% of HIF1α mRNA expression in SCC4 (Fig. 6; $p <$

0.001; n = 4) and 60% in SAS xenografts (Fig. S1A; $p < 0.05$; n = 4), whereas scrambled siRNA showed little effect. Thus, the observed therapeutic efficacy of HIF1α siRNA correlated well with RNAi of the target gene. Since the specimens were collected with combination PDT on day 10 after treatments, the protein expression profiles may not present the knockdown alone effect. In Fig. S1B, western blots of HIF1α knockdown effect in SAS xenografts were also examined. The amount of HIF1α protein decreased compared to PBS group in Fig. S1B.

In vivo antitumor H&E, CD31, Ki67, caspase-3, and TUNEL assay

To determine the biological effects of treatment with LCP HIF1α siRNA, tumors were harvested from mice following therapy and were subjected to hematoxylin and eosin (H&E) staining (Fig. 7), vessel marker (CD31), cellular proliferation (Ki67) and apoptosis (Caspase-3, TUNEL) (Fig. 8) assays. We also performed H&E staining of the liver and kidney from treated mice (Fig. 7) and no organ damage was observed. Hollow zones were seen in treated SCC4 and SAS tumor tissues, further supporting the conclusion that treatment with HIF1α siRNA in targeted LCP both with and without PDT reduced tumor volume (Figs. 7 and S2). Additionally, LCP HIF1α siRNA induced a significant decrease in CD31 and Ki67 staining, increased caspase-3 staining and increased response in the TUNEL assay in xenograft tumor tissues (Figs. 8 and S3). Body weight did not change significantly during the period of treatment (data not shown). In addition, quantification of the staining intensity of Ki67, caspase-3 and CD31 using image J software in Figs. 8A and S3A and the staining intensity of such biomarkers are shown in Figs. 8B and S3B, respectively. We observed that the major cause of tumor shrinkage is the mechanism of apoptosis due to the up-regulation of caspase-3, and the downregulation of Ki67 and CD31 in the therapeutic groups. We have used the 2° antibody only to do the negative controls for CD31 and Ki67 and the results in Figs. S9 and S10 showed low background.

Toxicity assay

All toxicity was assayed and analyzed using C57BL/6JNarl mouse serum. At the therapeutic dose (0.36 mg/kg), LCP did not induce significant levels of cytokines including interleukin-6 (IL-6) and IL-12 (Fig. S4). Levels of secreted liver biomarkers (aspartate aminotransferase (AST), alanine aminotransferase (ALT), total-Bilirubin (t-Bil)) (Fig. S5), kidney biomarkers (creatinine, blood urea nitrogen (BUN), calcium and phosphorus) (Fig. S6), albumin, total protein, globulin, glucose (Fig. S7) and muscle biomarkers (lactic dehydrogenase and creatine kinase) (Fig. S8) were all statistically unchanged in the serum after LCP HIF1α siRNA (3 times) treatment of normal C57BL/6JNarl black mice. This was consistent with the lack of damage to the liver, kidneys and muscles and unchanged calcium or phosphorus level in serum (n = 3).

Discussion

Although progress has been made, the 5-year survival rate for OSCC has not improved substantially in the past 10 years. Advances in tumor biology and understanding mechanisms of oncogenesis have revealed several potential molecular targets for OSCC treatment. We show here that a novel receptor-targeted delivery system (LCP) loaded with

siRNA targeting the HIF1α oncogene led to potent antitumor effects in OSCC. HIF1α is a core transcriptional factor of oxygen-suppressed (hypoxia) genes that mediate a wide range of adaptive responses to changes in oxygen tension in the tumor microenvironment. The center of solid tumors tends to be hypoxic enough to encourage angiogenesis and irregularities in vasculature and blood flow, likely contributing to rapid tumor growth [13,14]. Inhibition of the expression of this major hypoxic transcriptional factor by HIF1α RNAi is predictably effective in enhancement of tumor cell-killing effects, induction of apoptosis, and inhibition of tumor growth as shown by the current study.

CaP-based composite NPs have been recently developed for siRNA delivery [11,15,16]. These nanoparticles are effective for HIF1α siRNA delivery because the CaP can efficiently dissolve in the low pH microenvironment of the endosome and increase the osmotic pressure causing the endosome to swell and burst for a more consistent release of entrapped siRNA into the cytoplasm [12]. LCPs, CaP coated with lipid with target moiety (AA), are of a relatively small size (20–30 nm), biodegradable, biocompatible and have very low immunogenicity and non-toxic properties making them suitable for pre-clinical and clinical applications. In the present study, we have utilized lipid membrane coated CaP NP, i.e., the LCP [15], to deliver HIF1α siRNA in mouse OSCC models. SCC4 and SAS cells expressing sigma receptors were used as model cells in our *in vitro* and *in vivo* studies. During LCP formulation, the CaP core, stabilized with anionic lipid (DOPA), was prepared by using a reverse microemulsion synthetic approach and further coated with cationic lipid (DOTAP:cholesterol = 1:1). To prolong the *in vivo* circulation time and improve the cellular uptake, the final LCP was PEGylated with DSPE–PEG–AA. The LCP particles were 25–30 nm in diameter, which is a suitable size to be internalized by receptor-mediated endocytosis [17]. PEGylation on the nanoparticle surface could also maintain colloidal stability when redispersed after drying [18]. TEM revealed that LCPs were well dispersed with a hollow and spherical morphology and fairly uniform particle size (Fig. 2). Cabral et al. [19] reported that the enhanced delivery of drugs to tumor cells using nanoparticles mainly depends on size. They concluded that nanoparticles with a size smaller than 50 nm can penetrate poorly permeable tumors, such as pancreatic tumors. These findings support our LCP NP as suitable and sophisticated nanocarriers that enable efficient delivery and release of payloads to targeted cancer cells. Cellular uptake studies showed that the Texas Red-labeled dsDNAs were evenly distributed throughout the cytoplasm of SCC4 cells at 40 min post treatment when delivered by AA-targeted LCPs, while most untargeted LCPs remained attached to cell membranes without entering the cells or releasing Texas Red dye (Fig. 3). LCP-AA was able to successfully and efficiently deliver siRNA in a sigma receptor-mediated process (Fig. 3). IV injection of Texas Red-labeled HIF1α dsDNA formulated in LCPs led to preferential accumulation of the labeled dsDNA (3~5 fold increase in fluorescence intensity) throughout the cytoplasm of the whole tumor relative to major organs (Fig. 4), possibly because of higher passive transport of densely PEGylated lipid nanoparticles to leaky vessels of the tumor and extended blood circulation time. Additionally, AA may facilitate internalization, after which the pH-sensitive CaP core can disassemble in the acidic endosome and efficiently release the HIF1α dsDNA into the cytoplasm. In fact, Liu et al. [20] found fluorescence signals in LCP NP attenuated drastically in both liver and spleen organs compared to tumors based on a quantitative method. The issue may be caused by the

intrinsic tissue absorption and fluorescence light scattering effects. More attention is needed for the interpretation of LCP NP uptake using fluorescence-labeling dye.

PDT applications involve three major components including photosensitizer, light source and tissue oxygen. Photosan, a mixture of porphyrin oligomers, is intracellularly converted into the active photosensitizer, protoporphyrin IX (PpIX), in epithelial cells [21]. Reactive oxygen species generated can kill tumor cells directly or damage tumor-associated vasculature, leading to thrombus formation and subsequent tumor infarction.

For PDT of cancers of the head and neck, photosan is usually administered by intravenous injection (2 mg/kg) 48 h before the light treatment (total light dose, 100 J/cm2). A previous clinical study demonstrated that 51 of 57 patients with basal cell carcinoma, 6 of 7 patients with squamous cell carcinoma of the skin, 6 of 7 patients with oropharyngeal carcinoma, and 11 of 12 patients with laryngeal carcinoma showed a complete histologically confirmed response to a single course of PDT with systemic administration of photosan over a follow-up period of 13–71 months [22].

Recent studies have investigated the effects of PDT-induced hypoxia on the expression of proangiogenic factors and their relevance to treatment efficacy. Ferrario et al. [23] was the first to show that photofrin–PDT induces a modest increase in VEGF levels in BA carcinoma cells *in vitro*. They found that PDT performed on tumors *in vivo* resulted in HIF1α and VEGF upregulation. The results were consistent with Henderson and Donovan findings [24] showing that photofrin–PDT stimulates release of PGE_2 from macrophages and RIF tumor cells in culture and that the extent of release was dose dependent. Our experimental strategy was to knock down HIF1α gene expression before conducting PDT on OSCC tumors in order to investigate the efficacy of combined therapy.

In general, HIF1α siRNA formulated in LCP reduced HIF1α expression, increased apoptosis, inhibited proliferation of tumor cells, and enhanced photosan–PDT reduction in tumor volume. After treatment, microvascular CD31 and Ki67 immunostainings were significantly lower than in untreated tumors (Fig. 8), consistent with anti-angiogenic and anti-proliferative activities of HIF1α siRNA. LCP did not cause changes in host physiological profiles based on histopathological observation (Fig. 7). HIF1α siRNA formulated in LCP did not show any toxicity at the therapeutic dose, elicit any significant immune response (Fig. S4) and no organ toxicity was observed (Figs. S5–S8).

Previous researchers have reported that reactive oxygen species (ROS) play a crucial role in the regulation of HIF1α in a variety of cell types [25]. Sasabe et al. [26,27] studied how HIF1α influences the regulation of ROS generation and degradation in human OSCC. They reported that downregulation of HIF1α increases the intracellular levels of ROS in several human OSCC lines. In contrast, ROS production induced by chemotherapy agents was also decreased by the HIF1α expression vector transfected into oral squamous carcinoma cells-2 (OSC-2) and the anticancer agent-generated ROS amount was increased in the HIF1α siRNA duplex knockdown in human oral squamous carcinoma cells-5 (OSC-5). In the HIF1α knockdown OSCC cells, the expression of P-glycoprotein, heme oxygenase-1, manganese-superoxide dismutase and ceruloplasmin were downregulated and the

intracellular levels of chemotherapeutic drugs and ROS were sustained at higher levels after the treatment with the anticancer agents. Their findings are supportive to our conclusion that the downregulation of HIF1α is promoting ROS generation in cancer cells to enhance cell apoptosis via photodynamic therapy. Therefore, the combined silencing HIF1α gene therapy with photodynamic therapy could enhance PDT therapeutic outcome significantly. It suggests more ROS generated by downregulation of HIF1α could enhance ROS-mediated PDT therapeutic efficacy.

In summary, IV administered LCP could efficiently target the OSCC tumor to deliver therapeutic siRNA without presenting immunological or toxicological problems for the host. Systemic administration of HIF1α siRNA by targeted LCP appears to result in safe, stable, effective and sequence-specific inhibition of OSCC tumor growth at a relatively low siRNA dose (0.36 mg siRNA/kg body weight). Future experiments employing PDT prior to HIF1α siRNA in LCP and/or in combination with small-molecule drugs are likely to further enhance the antitumor potency of this system. We conclude that HIF1α siRNA formulated in LCP combined with PDT has the potential to emerge as an effective treatment for human OSCC.

Supplementary Material

Refer to Web version on PubMed Central for supplementary material.

Acknowledgments

We thank Srinivas Ramishetti for the synthesis of DSPE–PEG–AA. We thank Yang Liu for the help of animal technique including tail vein injection and biodistribution methods. We thank Steven Plonk and Andrew Blair for the assistance in manuscript editing. We thank Dr. CJ Liu for providing the SAS cell line. The work was supported by MOST grant 101-2221-E-033-001-MY2 and 103-2221-E-033-004, Taiwan. The work in Huang lab was supported by NIH grant CA149363.

Appendix: Supplementary material

Supplementary data to this article can be found online at doi:10.1016/j.canlet.2014.12.052.

References

1. Wamakulasuriya S. Global epidemiology if oral and oropharyngeal cancer. Oral Oncol. 2009; 45:309–316. [PubMed: 18804401]
2. Dolmans DE, Fukumura D, Jain RK. Photodynamic therapy for cancer. Nat Rev Cancer. 2003; 3:380–387. [PubMed: 12724736]
3. Grant WE, Hopper C, MacRobert AJ, Speight PM, Bown SG. Photodynamic therapy of oral cancer: photosensitisation with systemic aminolaevulinic acid. Lancet. 1993; 342:147–148. [PubMed: 7687318]
4. Fan KF, Hopper C, Speight PM, Buonaccorsi G, MacRobert AJ, Bown SG. Photodynamic therapy using 5-aminolevulinic acid for premalignant and malignant lesions of the oral cavity. Cancer. 1996; 78:1374–1383. [PubMed: 8839541]
5. Chen HM, Chen CT, Yang H, Lee MI, Kuo MY, Kuo YS, et al. Successful treatment of an extensive verrucous carcinoma with topical 5-aminolevulinic acid-mediated photodynamic therapy. J Oral Pathol Med. 2005; 34:253–256. [PubMed: 15752262]
6. Kalka K, Merk H, Mukhtar H. Photodynamic therapy in dermatology. J Am Acad Dermatol. 2000; 42:389–413. [PubMed: 10688709]

7. Dolmans DE, Kadambi A, Hill JS, Waters CA, Robinson BC, Walker JP, et al. Vascular accumulation of a novel photosensitizer, MV6401, causes selective thrombosis in tumor vessels after photodynamic therapy. Cancer Res. 2002; 62:2151–2156. [PubMed: 11929837]
8. Chiang CP, Huang WT, Lee JW, Hsu YC. Effective treatment of DMBA-induced hamster buccal cancer lesions by topical photosan-mediated photodynamic therapy. Head Neck. 2012; 34:505–512. [PubMed: 21484926]
9. Zhang Q, Zhang ZF, Rao JY, Sato D, Brown J, Messadi DV, et al. Treatment with siRNA and antisense oligonucleotides targeted to HIF-1α induced apoptosis in human tongue squamous cell carcinoma. Int J Cancer. 2004; 111:849–857. [PubMed: 15300796]
10. Hsu YC, Yang DF, Chiang CP, Lee JW, Tseng MK. Successful treatment of 7,12-dimethylbenz(a)anthracene-induced hamster buccal pouch precancerous lesions by topical 5-aminolevulinic acid-mediated photodynamic therapy. Photodiagnosis Photodyn Ther. 2012; 9:310–318. [PubMed: 23200011]
11. Yang Y, Li J, Liu F, Huang L. Systemic delivery of siRNA via LCP nanoparticle efficiently inhibits lung metastasis. Mol Ther. 2012; 20:609–615. [PubMed: 22186791]
12. Li J, Chen YC, Tseng YC, Mozumdar S, Huang L. Biodegradable calcium phosphate nanoparticle with lipid coating for systemic siRNA delivery. J Control Release. 2010; 142:416–421. [PubMed: 19919845]
13. Vaupel P, Kallinowski F, Okunieff P. Blood flow, oxygen and nutrient supply, and metabolic microenvironment of human tumors: a review. Cancer Res. 1984; 49:6449–6465. [PubMed: 2684393]
14. Höckel M, Vaupel P. Tumor hypoxia: definitions and current clinical, biologic, and molecular aspects. J Natl Cancer Inst. 2001; 93:266–276. [PubMed: 11181773]
15. Li J, Yang Y, Huang L. Calcium phosphate nanoparticles with an asymmetric lipid bilayer coating for siRNA delivery to the tumor. J Control Release. 2012; 158:108–214. [PubMed: 22056915]
16. Zhang M, Ishii A, Nishiyama N, Matsumoto S, Ishii T, Yamasaki Y, et al. PEGylated calcium phosphate nanocomposites as smart environment-sensitive carriers for siRNA delivery. Adv Mater. 2009; 21:3520–3525.
17. Huang L, Liu Y. *In vivo* delivery of RNAi with lipid-based nanoparticles. Annu Rev Biomed Eng. 2011; 13:507–530. [PubMed: 21639780]
18. Tabaković A, Kester M, Adair JH. Calcium phosphate-based composite nanoparticles in bioimaging and therapeutic delivery applications. Wiley Interdiscip Rev Nanomed Nanobiotechnol. 2012; 4:96–112. [PubMed: 21965173]
19. Cabral H, Matsumoto Y, Mizuno K, Chen Q, Murakami M, Kimura M, et al. Accumulation of sub-100 nm polymeric micelles in poorly permeable tumours depends on size. Nat Nanotechnol. 2011; 6:815–823. [PubMed: 22020122]
20. Liu Y, Tseng YC, Huang L. Biodistribution studies of nanoparticles using fluorescence imaging: a qualitative or quantitative method? Pharm Res. 2012; 29:3273–3277. [PubMed: 22806405]
21. Maier A, Tomaselli F, Matzi V, Woltsche M, Anegg U, Fell B, et al. Comparison of 5-aminolaevulinic acid and porphyrin photosensitization for photodynamic therapy of malignant bronchial stenosis: a clinical pilot study. Lasers Surg Med. 2002; 30:1–17. [PubMed: 11857597]
22. Feyh J. Photodynamic treatment for cancers of the head and neck. J Photochem Photobiol B, Biol. 1996; 36:175–177.
23. Ferrario A, Tiehl KF, Rucker N, Schwarz MA, Gill PS, Gomer CJ. Antiangiogenic treatment enhances photodynamic therapy responsiveness in a mouse mammary carcinoma. Cancer Res. 2000; 60:4066–4069. [PubMed: 10945611]
24. Henderson BW, Donovan JM. Release of prostaglandin E_2 from cells by photodynamic treatment *in vitro*. Cancer Res. 1989; 49:6896–6900. [PubMed: 2531034]
25. Kietzmann T, Gorlach A. Reactive oxygen species in the control of hypoxiainducible factor-mediated gene expression. Semin Cell Dev Biol. 2005; 16:474–486. [PubMed: 15905109]
26. Sasabe E, Tatemoto Y, Li D, Yamamoto T, Osaki T. Mechanism of HIF-1α-dependent suppression of hypoxia-induced apoptosis in squamous cell carcinoma cells. Cancer Sci. 2005; 96:394–402. [PubMed: 16053510]

27. Sasabe E, Zhou X, Li D, Oku N, Yamamoto T, Osaki T. The involvement of hypoxia-inducible factor-1α in the susceptibility to γ-rays and chemotherapeutic drugs of oral squamous cell carcinoma cells. Int J Cancer. 2006; 120:268–277. [PubMed: 17066447]

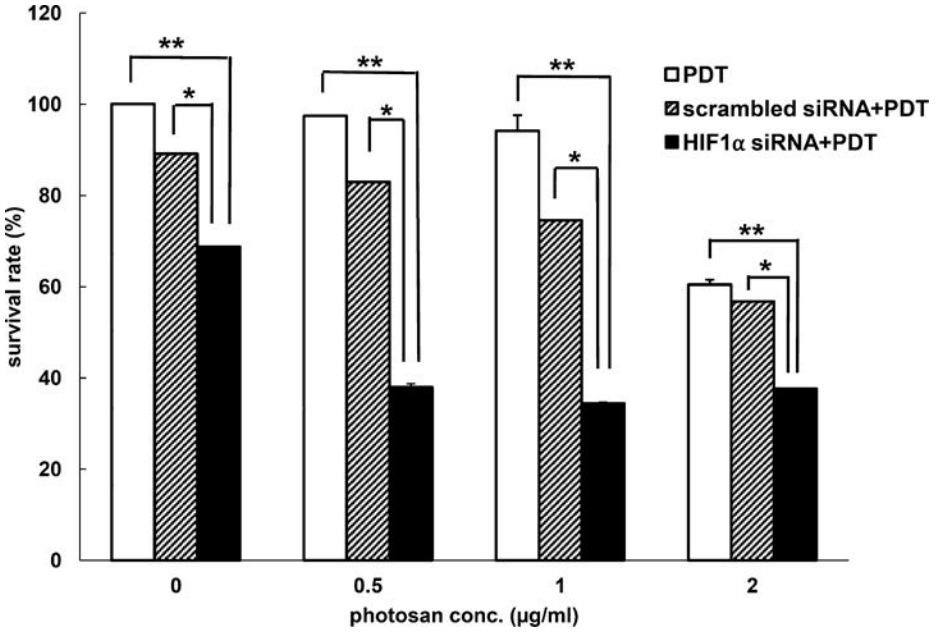

Fig. 1.

Effect of HIF1α siRNA gene therapy on anti-cancer effects of photodynamic therapy in cultured human SCC4 cells. Cells were treated with 50 nM HIF1α or scrambled siRNA to reduce HIF1α expression (not shown) and then subjected to photodynamic therapy using 0, 0.5, 1 and 2 μg/ml photosan at 24, 48 and 72 hrs after siRNA treatment. The percentage of surviving cells was measured by MTT assay as described and considered an indicator of anti-cancer effects of combined therapy. A significant difference ($p < 0.001$;**) in survival rate was seen between HIF1α siRNA/PDT (solid black bars) versus PDT alone (solid white bars). A significant difference ($p < 0.005$;*) in survival rate was seen between HIF1α siRNA/PDT (solid black bars) and scrambled siRNA/PDT (gray bars), while no significant difference was seen with scrambled siRNA (middle bar) when compared to PDT alone.

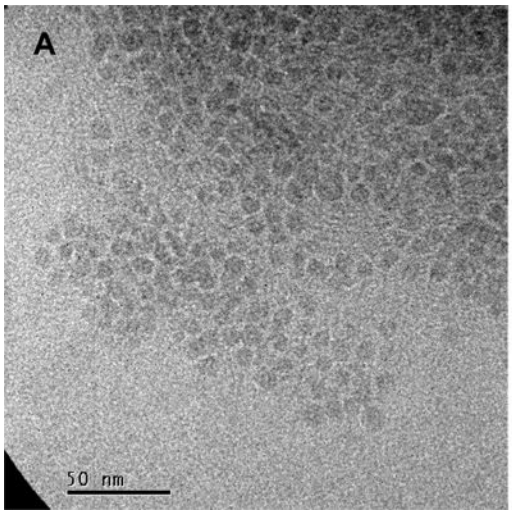

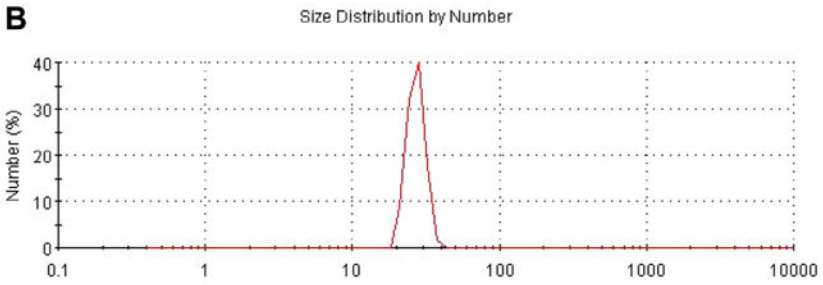

C Particle size of LCP

run	Particle size (nm)	Zeta Potential (mV)
1	25.4	43.3
2	27.8	45.5
3	30.5	46.7
Mean[a]	27.9 ± 2.6	45.2 ± 1.7

[a] mean ± standard deviation (n=3)

Fig. 2.

Characterization of LCP nanoparticles. (A) TEM imaging of LCP-HIF1α siRNA-AA was performed as described in *Materials and Methods*. (B) Size distribution of LCP HIF1α siRNA nanoparticles was determined as described. (C) Average LCP particle size and zeta potential of encapsulated HIF1α siRNA with AA was determined as described.

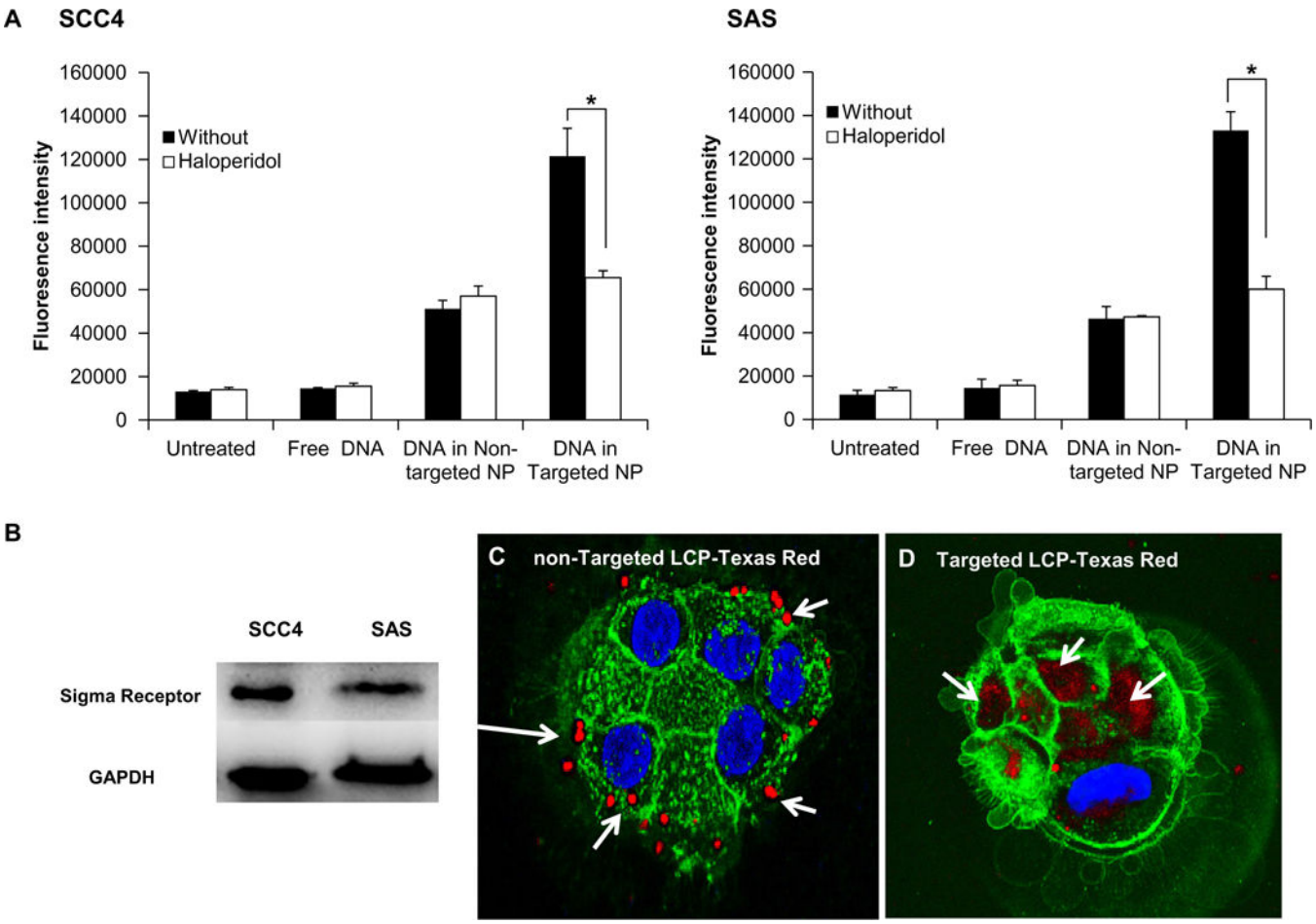

Fig. 3.

In vitro cellular uptake analysis of sigma receptor competition, existence of sigma receptors in OSCC cells and effect of anisamide targeting of LCP on sub-cellular distribution of delivered dsDNA cargo in cultured SCC4 cells. (A) Sigma receptor binding competition analysis of untreated, free DNA, DNA in non-targeted (no anisamide) LCP NP and DNA in targeted (with anisamide) LCP NP using haloperidol, the sigma receptor antagonist. (B) Western blots on examination of sigma receptor of SCC4 and SAS cell lines. (C, D) Texas Red-labeled HIF1α dsDNA was used as a model for siRNA and delivered to SCC4 cells using either AA-targeted or untargeted control LCP-PEG in order to investigate the effects of nanoparticle targeting on subcellular distribution of delivered cargo. Cells were visualized by confocal microscopy 40 minutes after LCP treatment. Nuclei were stained with DAPI (blue) and cell membranes were stained with wheat germ agglutinin (green). Arrows indicate the location of HIF1α dsDNA (red). (For interpretation of the references to color in this figure legend, the reader is referred to the web version of this article.)

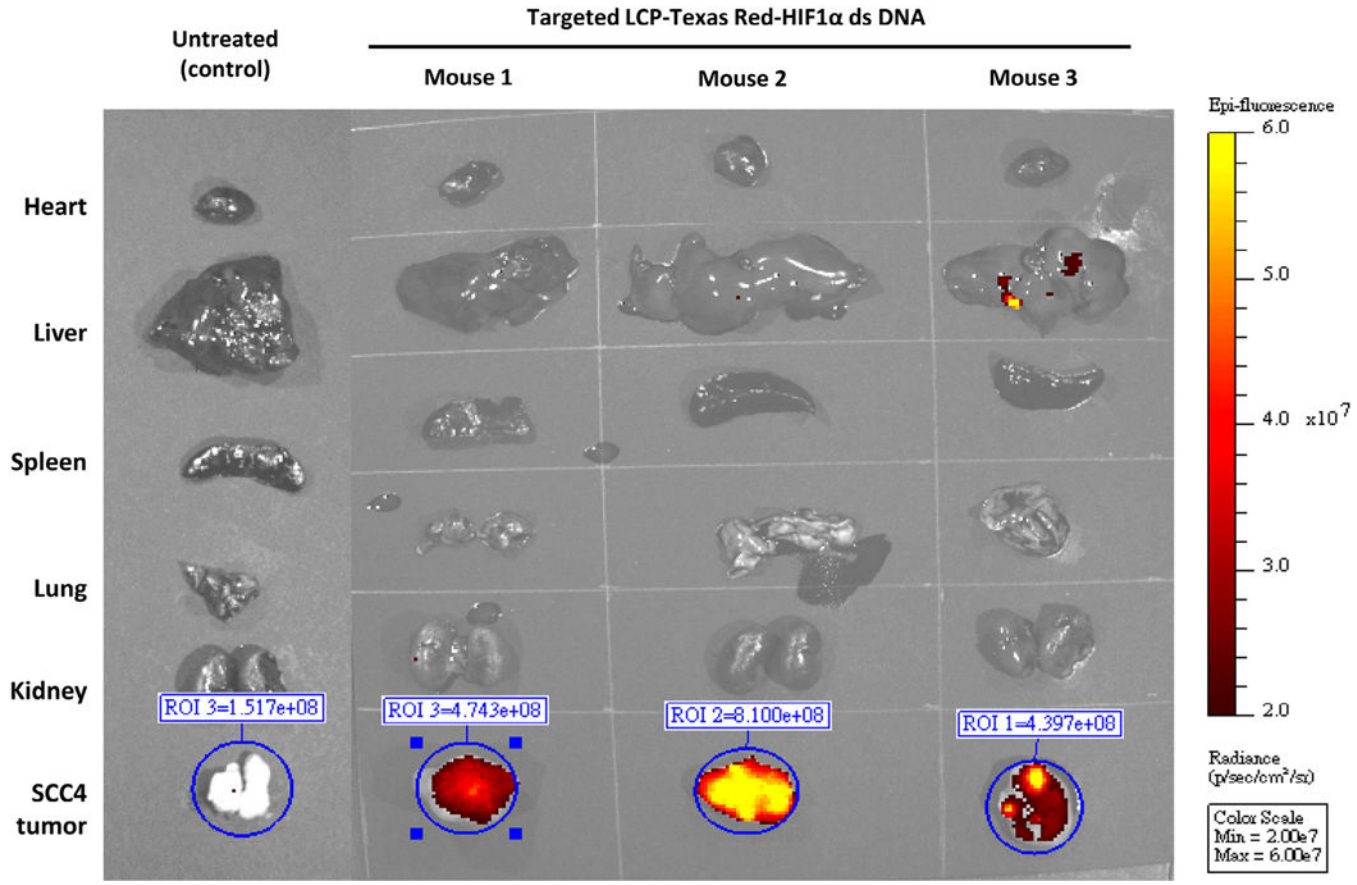

Fig. 4.

Bio-distribution of HIF1α dsDNA cargo after delivery by targeted LCP nanoparticles. SCC4 xenograft tumors reached 500–800 mm^3 and then mice were either left untreated (left) or intravenously injected with 6 μg LCP-Texas red-HIF1α dsDNA. Xenogen IVIS tumor imaging was performed 4 hours later as described.

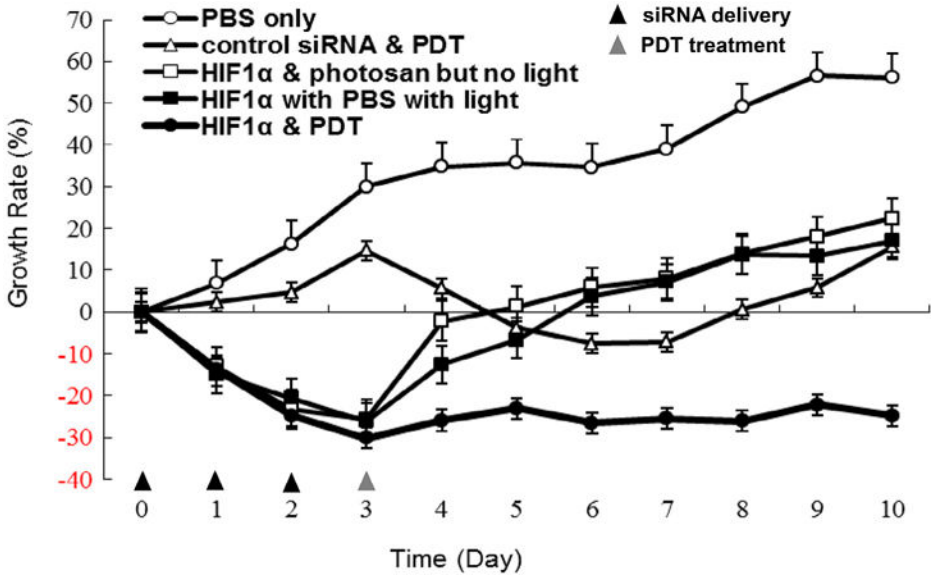

Fig. 5.

Effect of HIF1α siRNA delivered by targeted LCP nanoparticles on SCC4 tumor volume when combined with photodynamic therapy SCC4 xenograft tumors reached 500–800 mm^3 and then mice were intravenously injected on days 0, 1 and 2 with PBS (○) or 6 μg targeted LCP carrying either scrambled siRNA (△) or HIF1α siRNA (□, ■ and ●) followed by photosan (△, □ and ●) and light treatment (△, ■ and ●) on day 3. Tumors were measured daily as described to determine volume compared to day 0 and then converted to growth rate (%). Tumors were removed for pathological examination and q-PCR analysis on day 10.

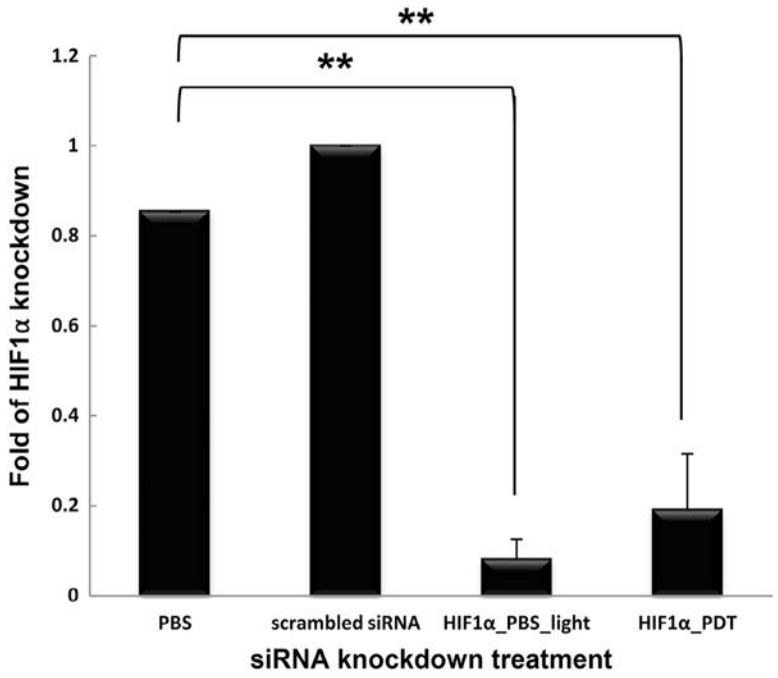

Fig. 6.

Effect of LCP-HIF1α siRNA on HIF1α mRNA levels in SCC4 xenograft tumor tissue. SCC4 xenograft tumor-bearing mice were intravenously injected with either PBS alone or targeted LCP nanoparticles carrying HIF1α siRNA on days 0, 1, and 2 followed by photosan and light treatment on day 3. Real-time quantitative PCR performed on day 10 revealed an 80% decrease in HIF1α mRNA level in siRNA-treated tumor tissue compared to PBS alone or scrambled siRNA (Student t-test, n = 4–8, $p < 0.001$).

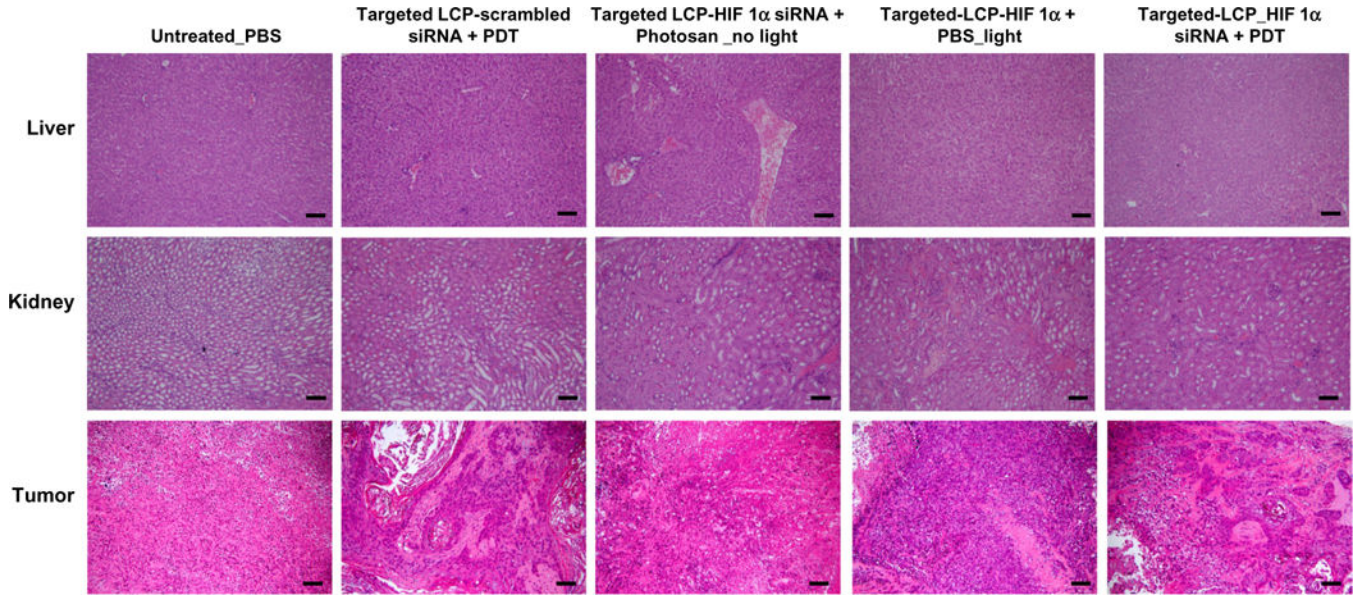

Fig. 7.

Hematoxylin and eosin-stained tissue sections from SCC4 xenograft tumor-bearing mice after treatment with targeted LCP-HIF1α siRNA. SCC4 xenograft tumors reached 500–800 mm^3 and then mice were intravenously injected on days 0, 1 and 2 with PBS or 6 μg LCP carrying either scrambled siRNA or HIF1α siRNA followed by photosan and light treatment on day 3. No major changes were observed in LCP-HIF1α siRNA treated liver and kidney tissue compared to scrambled siRNA or untreated tissue on day 10 after the start of treatment. However, major hollow areas were seen in tumor tissues treated with HIF1α siRNA. *Bar* standards for 100 μm.

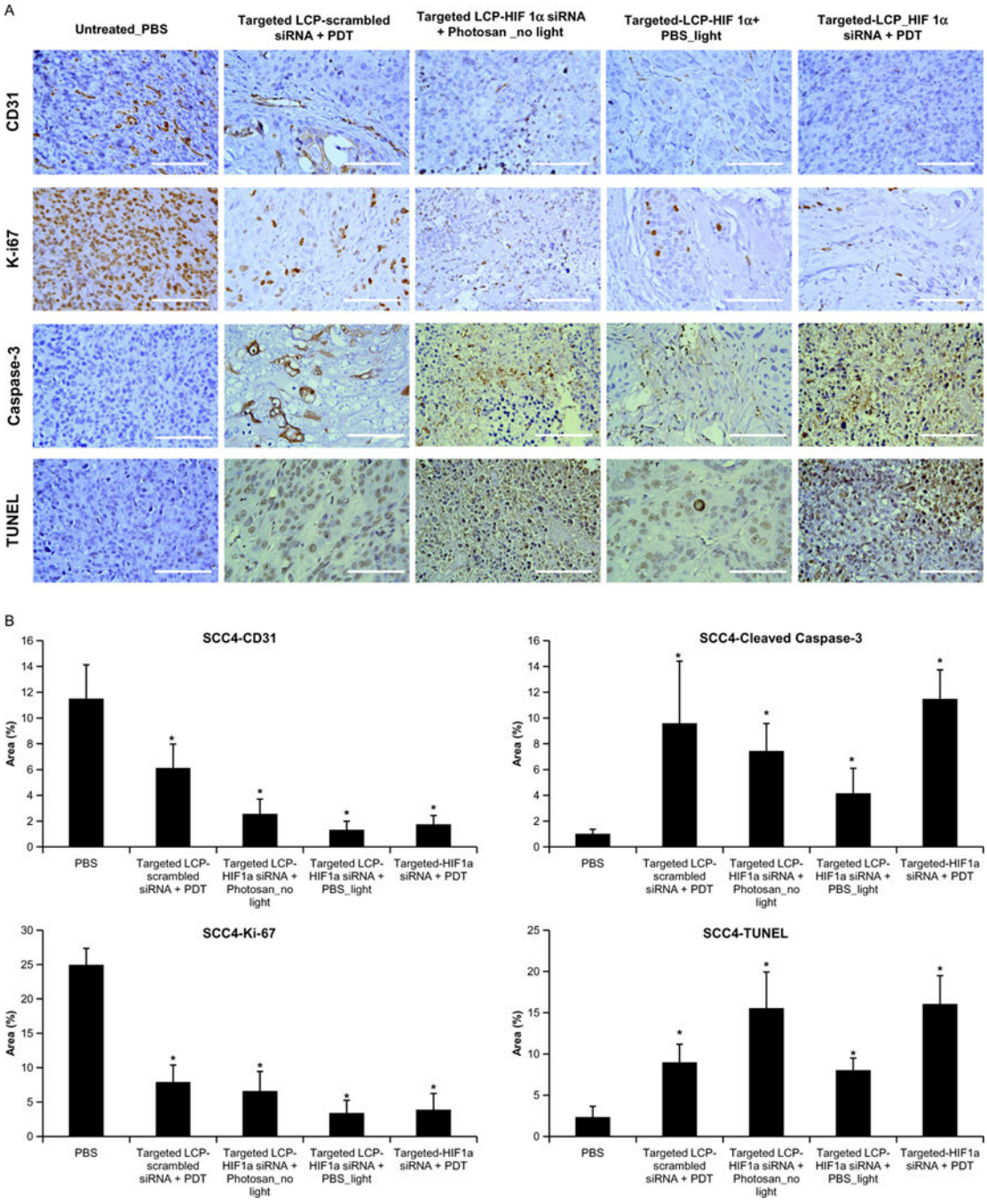

Fig. 8.

(a) Effect of targeted LCP-HIF1α siRNA on SCC4 xenograft tumor angiogenesis, proliferation and apoptosis. SCC4 xenograft tumors reached 500–800 mm^3 and then mice were intravenously injected on days 0, 1 and 2 with PBS or 6 μg LCP carrying either scrambled siRNA or HIF1α siRNA followed by photosan and light treatment on day 3. Immunohistochemical staining of tumor sections was then performed as described to determine effects on CD31 (brown), Ki67 (brown), caspase-3 (brown) and TUNEL assays (yellowish-red). *Bar* standards for 100 μm. (b) Quantification of the staining intensity of

CD31, Ki67 and caspase-3 using image J software in (a). (For interpretation of the references to color in this figure legend, the reader is referred to the web version of this article.)

Table 1A

Establishment of SCC4 xenograft mouse models for treatments.

Group	Experiments
1	PBS alone every 24 h for 3 days
2	LCP scramble siRNA (mock) every 24 h for 3 days and treated with PDT
3	LCP HIF1α siRNA every 24 hrs for 3 days and treated with photosan without light at the 4th day
4	LCP HIF1α siRNA every 24 hrs for 3 days and treated with PBS with light at the 4th day
5	LCP HIF1α siRNA every 24 hrs for 3 days and treated with PDT at the 4th day

Table 1B

Establishment of SAS xenograft mouse models for treatments.

Group	Experiments
1	PBS alone every 24 h for 3 days
2	LCP scrambled siRNA (mock) every 24 h for 3 days
3	LCP HIF1αsiRNA every 24 hrs for 3 days